The Meteoritical Society

Meteoritics & Planetary Science 1–14 (2018)
doi: 10.1111/maps.13062

Noble gas composition, cosmic-ray exposure age, ^{39}Ar-^{40}Ar, and I-Xe analyses of ungrouped achondrite NWA 7325

Jens HOPP[1,2*], Natalie SCHRÖTER[1], Olga PRAVDIVTSEVA[3], Hans-Peter MEYER[1], Mario TRIELOFF[1,2], and Ulrich OTT[1,4,5]

[1]Institut für Geowissenschaften, Universität Heidelberg, Im Neuenheimer Feld 234-236, D-69120 Heidelberg, Germany
[2]Klaus-Tschira-Labor für Kosmochemie, Im Neuenheimer Feld 234-236, D-69120 Heidelberg, Germany
[3]McDonnell Center for the Space Sciences and Physics Department of Washington University, One Brookings Drive, Saint Louis, Missouri 63130, USA
[4]MTA Atomki, Bem tér 18/c, 4026 Debrecen, Hungary
[5]Max-Planck-Institut für Chemie, Hahn-Meitner-Weg 1, D-55128 Mainz, Germany
[*]Corresponding author. E-mail: jens.hopp@geow.uni-heidelberg.de

(Received 29 June 2017; revision accepted 05 February 2018)

Abstract–Northwest Africa (NWA) 7325 is an anomalous achondrite that experienced episodes of large-degree melt extraction and interaction with melt under reducing conditions. Its composition led to speculations about a Mercurian origin and provoked a series of studies of this meteorite. We present the noble gas composition, and results of ^{40}Ar/^{39}Ar and ^{129}I-^{129}Xe studies of whole rock splits of NWA 7325. The light noble gases are dominated by cosmogenic isotopes. ^{21}Ne and ^{38}Ar cosmic-ray exposure ages are 25.6 and 18.9 Ma, respectively, when calculated with a nominal whole rock composition. This ^{38}Ar age is in reasonable agreement with a cosmic-ray exposure age of 17.5 Ma derived in our ^{40}Ar/^{39}Ar dating study. Due to the low K-content of 19 ± 1 ppm and high Ca-content of approximately 12.40 ± 0.15 wt%, no reliable ^{40}Ar/^{39}Ar age could be determined. The integrated age strongly depends on the choice of an initial ^{40}Ar/^{36}Ar ratio. An air-like component is dominant in lower temperature extractions and assuming air ^{40}Ar/^{36}Ar for the trapped component results in a calculated integrated age of 3200 ± 260 (1σ) Ma. This may represent the upper age limit for a major reheating event affecting the K-Ar system. Results of ^{129}I-^{129}Xe dating give no useful chronological information, i.e., no isochron is observed. Considering the highest ^{129}Xe*/^{128}Xe$_I$ ratio as equivalent to a lower age limit, we calculate an I-Xe age of about 4536 Ma. In addition, elevated ^{129}Xe/^{132}Xe ratios of up to 1.65 ± 0.18 in higher temperature extractions indicate an early formation of NWA 7325, with subsequent disturbance of the I-Xe system.

INTRODUCTION

The meteorite Northwest Africa (NWA) 7325 is a unique type of achondrite described as an iron-poor cumulate olivine gabbro which consists of the major mineral assemblage calcic plagioclase, diopside, and forsterite with accessory Cr-bearing iron sulfide and other opaque phases (Irving et al. 2013; Barrat et al. 2015). Soon after the first description of this rock speculations about its formation started, including a possible Mercurian origin (e.g., Irving et al. 2013) because of similarities with the surface composition of Mercury as determined by the MESSENGER spacecraft (Weider et al. 2012). As a result of the immediate interest raised by this meteorite, a rather large number of studies illuminated various aspects of mineralogy, petrology, chronology, and geochemistry of NWA 7325 (Amelin et al. 2013; Bischoff et al. 2013; Irving et al. 2013; Sanborn et al. 2013; Dunlap et al. 2014; El Goresy et al. 2014; Goodrich et al. 2014; Hasegawa

et al. 2014; Jabeen et al. 2014; Kita et al. 2014; Sutton et al. 2014; Weber et al. 2014, 2016; Barrat et al. 2015; Koefoed et al. 2016). The oxygen composition of NWA 7325 is similar to that of ureilites, but would also fit the winonaite and acapulcoite/lodranite trends (Irving et al. 2013) and hence, oxygen isotopic composition cannot provide an unequivocal genetic relationship with other achondrite groups. A genetic link to ureilites, however, appears unlikely due to the distinctive Cr isotopic pattern of NWA 7325 (Kita et al. 2014). On the basis of the oxygen isotopes, Jabeen et al. (2014) favored a planetary, though not explicitly Mercurian, origin of NWA 7325. Several chronologic studies established an ancient age of this meteorite. Its U-Pb age is 4562.5 ± 4.4 Ma (Amelin et al. 2013), indistinguishable from a Pb-Pb age of 4563.4 ± 2.6 Ma (Koefoed et al. 2016). Two reported ^{26}Al-^{26}Mg ages agree with these ages (4562.8 ± 0.3 Ma, Dunlap et al. 2014; 4563.09 ± 0.26, Koefoed et al. 2016). Such old ages argue against an origin from a large planetary body. Detailed petrographic descriptions are available from Bischoff et al. (2013), Irving et al. (2013), El Goresy et al. (2014), and Goodrich et al. (2014). Based on the texture of olivine grains, the assigned shock stage is S2 (Bischoff et al. 2013) but still allowing formation of plagioclase melt veins. However, Irving et al. (2013) proposed an impact-induced melting event that caused formation of reaction rims consisting of diopside around plagioclase in contact with olivine (Fig. 1). Trace element compositions of NWA 7325 are significantly depleted in lithophile and volatile trace elements (Barrat et al. 2015). The rare earth element composition resembles compositions found in lunar gabbroic/troctolitic meteorites, but show a much more pronounced Eu-anomaly than the latter (Irving et al. 2013; Barrat et al. 2015). Irving et al. (2013) concluded that NWA 7325 was formed as a cumulate rock from an unusual Fe-poor, Mg-Ca-rich silicate magma at high temperatures and low oxygen fugacity approaching conditions assumed for enstatite chondrite formation. In addition, Barrat et al. (2015) argued for a two-stage melting process in order to explain the unusual major and minor element patterns. In their view, the cumulate rock NWA 7325 is the product of a second melting episode of gabbroic material, e.g., induced by an impact event. If so, the observed ages only would apply to this second event and hence, postdate the formation of NWA 7325 by perhaps several millions of years. Thus, NWA 7325 might be the oldest preserved crustal material of an achondritic parent body (Barrat et al. 2015). Xenon isotopic compositions in stepwise heating experiments were provided by Weber et al. (2016). At high extraction temperatures, they observed elevated ^{129}Xe/^{132}Xe ratios presumed to be a consequence of ^{129}I decay. Furthermore, these authors found evidence of modest contributions of ^{129}Xe from iodine decay released at intermediate temperatures. Provided these temperature steps are related to extraction of a rehomogenized ^{129}Xe/^{132}Xe component, the respective slightly elevated ^{129}Xe/^{132}Xe ratios could point to later processing of the rock allowing for substantial decay of ^{129}I during several tens of million years (Weber et al. 2016). ^{39}Ar-^{40}Ar ages agree with an early formation (Weber et al. 2016), but show large uncertainties due to the low K-content of NWA 7325. Within the same study, cosmic-ray exposure ages of 18–19 Ma were obtained via the Ar-Ar method. In this approach, cosmogenic ^{38}Ar is determined within an Ar-Ar analysis, while the Ca-content of the sample is obtained from the amount of reactor-produced ^{37}Ar during neutron reaction with ^{40}Ca. The calculation of a CRE age is then based on the (almost) correct assumption that Ca is the major target for $^{38}Ar_{COS}$ production (in case of NWA 7325 with its high Ca-content, more than 99% are from Ca; see the Cosmic-Ray Exposure Age Derived by $38Ar/37Ar_{Ca}$ Ratios section). A similar cosmic-ray exposure age of 20 Ma was reported in a conference abstract by Hasegawa et al. (2014) on the basis of cosmogenic ^{3}He and ^{21}Ne. In addition, these authors found elevated ^{129}Xe/^{132}Xe ratios up to 2.6. From that, they argued for an early degassing event, followed by subsequent fast cooling, at a time when ^{129}I was still alive.

Here we report the noble gas composition of NWA 7325 and determine its cosmic-ray exposure age. In addition, we performed a ^{40}Ar/^{39}Ar dating study which potentially allows assessing the absolute age of formation or the (e.g., impact-induced) last heating event related to the history of NWA 7325, though we are aware of the problems of low precision ages due to low K-contents. Furthermore, Ar-Ar dating also enables calculating a cosmic-ray exposure age. Eventually, we performed a ^{129}I-^{129}Xe analysis to check for additional age constraints.

SAMPLE AND EXPERIMENTAL DETAILS

A ~1 g slice of NWA 7325 was purchased from the main mass holder Stefan Ralew (Berlin, Germany). According to Irving et al. (2013), the bulk major element composition of NWA 7325 is (in wt%) SiO_2 47.09, TiO_2 0.01, Al_2O_3 18.60, Cr_2O_3 0.40, FeO 1.57, MnO 0.03, MgO 12.13, CaO 17.94, Na_2O 0.60, K_2O 0.01, and P_2O_5 0.02.

A small piece was prepared for analysis with the electron microprobe (Cameca SX 51). These analyses were conducted with an electron beam energy of 15 kV and 20 nA sample current. Results are provided as

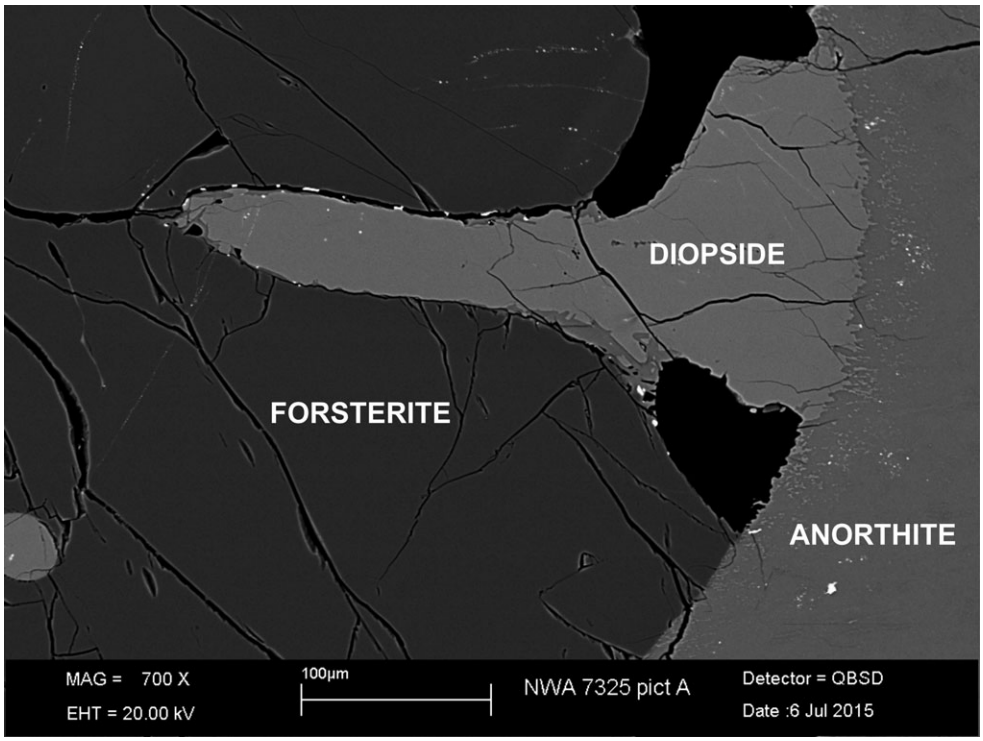

Fig. 1. Backscattered electron microscope picture of NWA 7325 showing the major minerals forsterite, diopside, and anorthite. Bright spots of opaque minerals consist predominantly of troilite. Diopside apparently occupies the volume of a former melt pocket and shows a reaction rim with anorthite.

Supplementary Material 1 in supporting information, and backscattered electron pictures of the whole thin section are added in Supplementary Material 2 in supporting information.

For noble gas analyses, mm-sized parts of the interior of the slice were removed by gentle grinding and cleaned with high-purity ethanol in an ultrasonic bath. After drying, the whole rock pieces were wrapped in high-purity Al-foil. Two larger pieces were used for noble gas analyses, and a smaller one for Ar-Ar dating.

Ar-Ar Dating

The sample for Ar-Ar dating was placed within an evacuated quartz ampoule (approximately 10^{-1} mbar) and neutron-irradiated with Cd-shielding at the Portuguese Research Reactor in Bobadela for 96 h (total fast neutron flux approximately 10^{18} n cm^{-2}). Irradiation was interrupted frequently due to the reactor schedule, which made a corresponding decay correction necessary for ^{37}Ar (correction on ^{39}Ar was negligible compared to the total uncertainty of analyses). Two NL25 hornblende age monitors (monitor age 2.657 ± 0.004 Ga; Schwarz and Trieloff 2007) bracketed the meteorite in the sample vial. In addition, a CaF_2 standard yielded information about necessary interference corrections to Ar from nuclear reactions on Ca. The following interference parameters from Ca and K were used for correction: $(^{36}Ar/^{37}Ar)_{Ca}$ = 0.0026 ± 0.0024; $(^{39}Ar/^{37}Ar)_{Ca}$ = 0.00099 ± 0.00004; $(^{40}Ar/^{37}Ar)_{Ca}$ = 0.003 ± 0.003 (Turner 1971); $(^{38}Ar/^{39}Ar)_{K}$ = 0.0107 ± 0.0020; $(^{40}Ar/^{39}Ar)_{K}$ = 0.0123 ± 0.0024 (Brereton 1970).

Gas extraction was performed by stepwise heating using an inductively heated furnace with a Mo-crucible. Each gas fraction was cleaned by two hot (about 400 °C) and one cold Al-Zr-Getter prior to measurement. Ar isotopic compositions were determined with an in-house modified Varian MAT CH5 mass spectrometer. Frequent determination of calibration gas with air composition was used to correct for instrumental mass fractionation. We measured blanks at several temperatures. Respective blank heights followed an exponential relationship with temperature. The isotopic composition of blanks was indistinguishable from air composition within error. ^{37}Ar and ^{39}Ar from the blank gas measurements were averaged and subtracted. For evaluation we used the recommended decay constants from Steiger and Jäger (1977). Note that the decay constants are currently in revision and

most widely accepted alternative values would increase the reported ages in the age range of 3.0-4.5 Ga by about 10-30 Ma (Renne et al. 2011; Schwarz et al. 2011). Results are provided in Supplementary Material 3 in supporting information.

Iodine–Xenon Analyses

A whole rock split of 73.80 mg was prepared for I-Xe analyses by cleaning with pure ethanol and deionized water in an ultrasonic bath.

This split, along with the Shallowater aubrite absolute age standard (4562.4 ± 0.2 Ma; Pravdivtseva et al. 2017a, 2017b), was irradiated with thermal neutrons as part of the SLC–18 capsule in the Missouri University Research Reactor (MURR), receiving $\approx 2 \times 10^{19}$ neutrons cm^{-2}. The samples were placed in a fixed horizontal plane at the center of the vertical neutron profile in the reflector area of the reactor to minimize any vertical gradient and the capsule was continuously rotated to eliminate any *x*–*y* gradient. After cooling, samples were removed from the quartz ampoules, wrapped in platinum foil, and placed in the extraction system of the mass spectrometer.

Xenon was released in stepwise extractions in a W-coil; released gases were cleaned sequentially by first exposing them to SAES St707 getter pellets maintained at 275 °C, and then to freshly deposited Ti-film getters. The heavy noble gases were separated from helium, neon, and argon using activated charcoal at a temperature of −90 °C for adsorption of xenon (the light gases were pumped away) and +165 °C for xenon desorption. The isotopic composition of the released xenon was measured by high transmission ion-counting mass spectrometry (Hohenberg 1980). Hot blanks were measured with an empty coil at 1500 °C (15 min) following standard analytical procedures equivalent to sample measurements and were about 2×10^{-15} cm^3 STP of ^{132}Xe and approximately atmospheric in composition. Sensitivity of the spectrometer corresponded to 8.1×10^{-16} cm^3 STP/(count per second). Results of the I-Xe measurements are given in Table 1.

Noble Gas Analyses

Noble gas analyses of two whole rock splits (NWA 7325 wr1 and wr2) were performed with an in-house modified VG3600 mass spectrometer at Institut für Geowissenschaften, University of Heidelberg, Germany. A detailed summary of the experimental procedures is given in Supplementary Material 4 in supporting information. Results of noble gas analyses are summarized in Tables 2 (He, Ne, Ar), 3 (Kr, only NWA 7325 wr1), and 4 (Xe).

RESULTS AND DISCUSSION

Electron Microprobe Data

We analyzed the major phases olivine, diopside, and plagioclase, and troilite. All compositions can be found in Supplementary Material 1. The average compositions of olivine ($Fo_{96.7}$), diopside ($En_{53.3}$ $Fs_{1.3}$ $Wo_{45.5}$), plagioclase ($An_{88.8}$), and troilite (2.9 wt% Cr, 0.27 wt% Ni) agree well with the range reported by Irving et al. (2013) and Barrat et al. (2015). Large grains of adjacent forsterite, diopside, and anorthite with minute grains of opaque troilite are shown in a backscattered electron microscope image (Fig. 1) documenting the replacement of anorthite within a reaction zone by a diopsidic melt (e.g., Irving et al. 2013). The melt formation might be due to an impact-induced thermal event, but alternatively could also result from parent body processes.

Ar-Ar Dating

The very low ^{39}Ar concentration (produced by the reaction $^{39}K(n,p)^{39}Ar$) and hence, K-content of the sample of 19 ± 1 ppm is remarkable (Supplementary Material 3). In part, this might be an artifact of Ca interference corrections which are strongly reducing the $^{39}Ar_K$ net signal. For example, at 1400 °C after correction for production by neutron reactions on Ca (major reactions with Ca are $^{40}Ca[n,\alpha]^{37}Ar$ and $^{42}Ca[n,\alpha]^{39}Ar$), no ^{39}Ar is left. Because of the huge Ca signal at higher temperatures, a small systematic error in the respective interference ratio determined with a CaF_2 standard could change the true K-derived $^{39}Ar_K$ signal significantly. For example, allowing for a 10% lower interference ratio of $(^{39}Ar/^{37}Ar)_{Ca}$ (which would approximately represent the lower 2σ-uncertainty value of this ratio) would leave a small residual amount of $^{39}Ar_K$ in the 1400 °C extraction (at the major ^{37}Ar release peak), which otherwise disappears. However, even allowing for some overcorrection, it is clear that the K-content is low. Similarly, the Ca correction to ^{36}Ar is large, but cannot compete with the high cosmogenic proportion which is indicated by the high $^{38}Ar/^{36}Ar$ ratios rising continuously from about 0.23 to 1.55, the lower value resulting from addition of dominantly atmospheric argon in low-temperature extractions and the higher value closely approximating the cosmogenic production ratio. Apparently, the initial argon component within the sample (i.e., that not produced during neutron-irradiation) is characterized by significant amounts of cosmogenic argon. This compares well with the results of the noble gas analyses (see the Noble Gas Composition and CRE-Ages From

Table 1. Xe isotopic compositions of anomalous achondrite NWA 7325, irradiated sample. No correction for spallation and ^{235}U fission is applied.

NWA 7325 wr, 73.80 mg										
Temperature (°C)	^{132}Xe 10^{-11} cm^3 STP g^{-1}	^{124}Xe	^{126}Xe	^{128}Xe	^{129}Xe	^{130}Xe	^{131}Xe	^{132}Xe = 100	^{134}Xe	^{136}Xe
800	0.2145	0.258 ± 0.040	0.669 ± 0.078	65005 ± 675	68.02 ± 1.29	8.06 ± 0.31	1934 ± 20	100 ± 0	107.9 ± 1.6	145.9 ± 2.0
1000	0.7745	−0.002 ± 0.039	0.713 ± 0.200	98902 ± 1623	39.51 ± 1.09	1.36 ± 0.12	3007 ± 70	100 ± 0	165.0 ± 3.2	243.2 ± 3.0
1100	0.1999	0.325 ± 0.054	0.479 ± 0.064	11635 ± 91	77.85 ± 1.25	11.87 ± 0.35	11677 ± 103	100 ± 0	75.7 ± 1.4	92.4 ± 1.3
1200	0.3043	0.263 ± 0.035	0.393 ± 0.056	5420 ± 32	75.05 ± 0.95	11.29 ± 0.29	2414 ± 14	100 ± 0	81.7 ± 1.1	103.0 ± 1.0
1250	0.1949	0.230 ± 0.062	0.196 ± 0.052	3740 ± 30	58.43 ± 0.91	8.40 ± 0.31	1651 ± 19	100 ± 0	111.9 ± 0.9	150.2 ± 2.0
1300	0.1603	0.164 ± 0.063	0.207 ± 0.079	2316 ± 23	69.99 ± 0.86	7.75 ± 0.33	1983 ± 21	100 ± 0	109.7 ± 1.9	147.4 ± 1.5
1350	0.4803	0.235 ± 0.038	0.223 ± 0.034	1017 ± 7	83.14 ± 0.69	8.80 ± 0.19	2104 ± 14	100 ± 0	104.3 ± 0.9	141.6 ± 1.3
1400	1.263	0.286 ± 0.024	0.314 ± 0.023	474.3 ± 2.8	104.28 ± 0.58	10.81 ± 0.15	1189 ± 4	100 ± 0	85.3 ± 0.5	109.0 ± 0.8
1450	1.482	0.422 ± 0.031	0.368 ± 0.024	144.8 ± 1.0	127.22 ± 0.59	14.61 ± 0.18	627.8 ± 2.9	100 ± 0	52.9 ± 0.2	56.0 ± 0.5
1500	0.008710	0.910 ± 0.367	0.165 ± 0.358	230.9 ± 13.0	125.53 ± 7.84	16.54 ± 1.99	407.4 ± 19.4	100 ± 0	50.6 ± 3.4	42.8 ± 4.1
1525	0.002666	0.692 ± 0.786	1.043 ± 0.841	266.1 ± 35.3	95.77 ± 11.14	9.15 ± 2.21	335.8 ± 29.7	100 ± 0	37.9 ± 7.4	36.7 ± 7.2
1550	0.002919	−1.046 ± 0.576	−0.002 ± 0.738	227.0 ± 29.4	112.51 ± 9.18	13.35 ± 2.91	186.7 ± 17.3	100 ± 0	33.1 ± 5.2	39.1 ± 2.7
1600	0.005103	0.516 ± 0.416	0.093 ± 0.346	129.4 ± 15.4	92.29 ± 6.5	9.82 ± 1.89	160.7 ± 12.8	100 ± 0	40.7 ± 4.7	34.2 ± 4.5
1650	0.008954	0.548 ± 0.338	−0.039 ± 0.270	92.0 ± 8.7	100.11 ± 5.74	15.14 ± 1.99	98.3 ± 8.4	100 ± 0	40.5 ± 2.9	30.0 ± 3.4
1700	0.01537	0.471 ± 0.292	0.881 ± 0.162	46.9 ± 5.2	99.24 ± 4.83	18.61 ± 1.63	97.9 ± 5.2	100 ± 0	40.9 ± 2.7	34.1 ± 1.7
1750	0.02275	−0.066 ± 0.137	0.514 ± 0.181	40.8 ± 2.4	102.59 ± 3.06	16.76 ± 1.07	84.5 ± 3.9	100 ± 0	41.0 ± 2.0	37.7 ± 2.4
1850	0.09897	0.316 ± 0.065	0.435 ± 0.103	18.4 ± 1.3	101.42 ± 1.33	14.94 ± 0.56	81.5 ± 1.9	100 ± 0	38.6 ± 0.9	33.7 ± 1.2
1900	0.1792	0.371 ± 0.071	0.297 ± 0.061	15.9 ± 0.9	97.86 ± 1.1	15.29 ± 0.37	79.4 ± 1.4	100 ± 0	40.2 ± 0.6	33.6 ± 0.6
Total	5.382	0.297 ± 0.013	0.372 ± 0.019	18010 ± 275	96.72 ± 0.3	11.12 ± 0.08	1737 ± 9	100 ± 0	82.5 ± 0.4	104.6 ± 0.4
AIR[a]		0.3537 ± 0.0011	0.3300 ± 0.0017	7.136 ± 0.009	98.32 ± 0.12	15.136 ± 0.012	78.90 ± 0.11	100 ± 0	38.79 ± 0.06	32.94 ± 0.04
OC-Xe[b]		0.4633 ± 0.0055	0.4127 ± 0.0033	8.271 ± 0.041	103.99 ± 0.25	16.198 ± 0.045	81.95 ± 0.20	100 ± 0	37.96 ± 0.11	31.80 ± 0.06

[a]After Ozima and Podosek (1983).
[b]After Lavielle and Marti (1992).

Table 2. He, Ne, and Ar isotopic compositions of ungrouped achondrite NWA 7325.

Extraction	^{4}He (10^{-9})[a]	^{3}He (10^{-10})[a]	^{4}He/^{3}He	^{22}Ne (10^{-11})[a]	^{20}Ne/^{22}Ne	^{21}Ne/^{22}Ne	^{36}Ar (10^{-11})[a]	^{38}Ar/^{36}Ar	^{40}Ar/^{36}Ar
NWA 7325 wr1; 200.2 mg									
800 °C	153 (4)	232 (5)	6.60 (22)	200 (1)	0.761 (4)	0.799 (11)	9.18 (67)	0.445 (21)	295 (13)
1200 °C	716 (6)	960 (19)	7.46 (16)	2686 (4)	0.774 (1)	0.842 (11)	469 (10)	1.430 (14)	64.0 (3)
1350 °C	23.5 (1.8)	27.5 (5)	8.52 (69)	78.7 (1.1)	0.751 (10)	0.921 (18)	449 (9)	1.470 (6)	40.5 (4)
1550 °C	3.3 (1.8)	1.46 (3)	23 (12)	187 (1)	0.851 (5)	0.928 (13)	90.4 (1.8)	1.475 (8)	76.8 (2.0)
1800 °C	11.7 (1.8)	0.044 (2)	2635 (432)	16.0 (0.6)	2.36 (8)	0.766 (36)	19.2 (1.2)	1.672 (83)	64 (20)
Total	908 (8)	1221 (19)	7.43 (14)	3167 (5)	0.785 (7)	0.846 (7)	1037 (14)	1.447 (30)	57.0 (9)
NWA 7325 wr2; 57.9 mg									
1000 °C	1199 (41)	1762 (14)	6.80 (24)	3102 (5)	0.694 (1)	0.786 (1)	388 (10)	0.534 (6)	283 (4)
1800 °C	371 (14)	445 (3)	8.33 (33)	4221 (6)	0.975 (1)	0.854 (1)	2787 (58)	1.518 (9)	48.4 (7)
1800 °C (2^{nd})	10 (9)	0.020 (2)	4897 (4636)	12.0 (4)	8.52 (26)	0.118 (4)	260 (8)	0.252 (3)	339 (5)
Total	1579 (44)	2207 (14)	7.16 (20)	7334 (8)	0.868 (3)	0.824 (3)	3434 (60)	1.311 (35)	96.9 (2.3)

Errors in parentheses refer to the last significant digits and represent 1σ-uncertainties.
[a]In cm^3 STP g^{-1}.

Table 3. Kr isotopic compositions of ungrouped achondrite NWA 7325.

Extraction[a]	^{84}Kr (10^{-13})[b]	^{82}Kr/^{84}Kr	^{83}Kr/^{84}Kr	^{86}Kr/^{84}Kr
NWA 7325 wr1; 200.2 mg				
1200 °C	211 (20)	0.284 (5)	0.305 (5)	0.275 (5)

Errors in parentheses refer to the last significant digits and represent 1σ-uncertainties.
[a]Only 1200 °C extraction above blank level.
[b]In cm^3 STP g^{-1}.

Cosmogenic 3He, 21Ne, and 38Ar Abundances in Nonirradiated Whole Rock Splits section).

The significant corrections applied to the age calculations cause large uncertainties, which are documented in the age spectra in Fig. 2A. The integrated age of NWA 7325 wr is 4435 ± 87 Ma (1σ-error), if we assume a ^{40}Ar/^{36}Ar composition of 1 ± 1 (equivalent to a solar value) of the initial (i.e., non-radiogenic and non-cosmogenic, commonly termed trapped) argon component present at the time of isotopic closure (black age spectrum in Fig. 2A), while neglecting the ^{40}Ar concentration in the 1400 °C extraction which showed no $^{39}Ar_K$ after Ca interference correction (see above). This would agree with Ar-Ar ages given by Weber et al. (2016) who report ages of 4300-4500 Ma. These authors derived initial ^{40}Ar/^{36}Ar ratios of 6.7 ± 6.9 and 3 ± 13, similar to a solar Ar component, suggesting our assessed choice of an initial ^{40}Ar/^{36}Ar = 1 ± 1 would be a good approximation. However, a closer look reveals clear differences in isotopic composition between lower temperature extractions (500–900 °C) and higher temperature extractions (>900 °C). At lower temperatures, ^{36}Ar/^{38}Ar ratios are >2 (equivalent to more than 28.9% trapped, non-cosmogenic ^{38}Ar) and ^{40}Ar/^{36}Ar ratios are approximately atmospheric in composition, whereas at higher temperatures, ^{36}Ar/^{38}Ar ratios are <1 (equivalent to <7.4% trapped ^{38}Ar). The most likely explanation of this observation is a substantial incorporation of atmospheric argon as a result of weathering processes in the desert that is mainly observed in the low-temperature extractions. Note that the trace element budget in NWA 7325 also supports an influence of desert weathering (Barrat et al. 2015). It is thus likely that a significant amount of atmospheric ^{40}Ar is present in these extractions whose inclusion in the calculation of an integrated age is not justified and hence, the integrated age given above is significantly overestimated, as also seen in the comparison of age spectra in Fig. 2A (corrected with a solar ^{40}Ar/^{36}Ar ratio: black; corrected with an atmospheric ^{40}Ar/^{36}Ar ratio: gray). Further evidence for the presence of air Ar comes from the three-isotope diagram of Fig. 2B, where all data points fall along or slightly above a mixing line between atmospheric and cosmogenic argon (with $^{40}Ar/^{36}Ar_{ATM}$ = 295.5 ± 0.5; $^{38}Ar/^{36}Ar_{ATM}$ = 0.1885 ± 0.0003; $^{40}Ar/^{36}Ar_{COS}$ = 0.308 ± 0.154; $^{38}Ar/^{36}Ar_{COS}$ = 1.538 ± 0.047; Lämmerzahl and Zähringer 1966; Steiger and Jäger 1977; Lee et al. 2006). There is no evidence of a solar or planetary argon component with a composition below the mixing trend. If we only regard excess ^{40}Ar relative to the mixing trend being truly radiogenic, the respective ^{40}Ar/^{39}Ar age reduces to 3200 ± 260 Ma (again, excluding the 1400 °C extraction). Since, nevertheless, minor undetected amounts of solar or planetary argon may have been present in the sample, this age represents a minimum age. The integrated age of 3200 ± 260 Ma presumably marks the upper age limit of a late, possibly impact-induced, heating event. Evidently, this is in contrast to the old Ar-Ar ages reported by Weber

Table 4. Xe isotopic compositions of ungrouped achondrite NWA 7325.

Extraction[a]	^{132}Xe (10^{-14})[b]	$^{124}Xe/^{132}Xe$	$^{126}Xe/^{132}Xe$	$^{128}Xe/^{132}Xe$	$^{129}Xe/^{132}Xe$
NWA 7325 wr 1; 200.2 mg					
1200 °C	968 (268)	0.0073 (12)	0.0049 (18)	0.086 (7)	1.49 (6)
	$^{130}Xe/^{132}Xe$	$^{131}Xe/^{132}Xe$	$^{134}Xe/^{132}Xe$	$^{136}Xe/^{132}Xe$	
1200 °C	0.163 (11)	0.84 (5)	0.373 (22)	0.294 (18)	
NWA 7325 wr 2; 57.9 mg					
1000 °C	736 (80)	0.0040 (23)	0.0048 (18)	0.092 (17)	1.07 (16)
1800 °C	3096 (239)	0.0042 (10	0.0041 (8)	0.088 (10)	1.65 (18)
1800 °C (2nd)	87 (71)	0.074 (95)	0.029 (39)	0.06 (10)	0.58 (63)
Total	3919 (262)	0.0057 (19)	0.0048 (10)	0.088 (9)	1.52 (14)
	$^{130}Xe/^{132}Xe$	$^{131}Xe/^{132}Xe$	$^{134}Xe/^{132}Xe$	$^{136}Xe/^{132}Xe$	
1000 °C	0.141 (24)	1.01 (16)	0.357 (58)	0.343 (60)	
1800 °C	0.166 (19)	0.87 (10)	0.363 (42)	0.320 (39)	
1800 °C (2nd)	0.040 (69)	0.63 (76)	0.16 (21)	0.11 (16)	
Total	0.158 (16)	0.90 (9)	0.357 (36)	0.320 (33)	

Errors in parentheses refer to the last significant digits and represent 1σ-uncertainties.
[a]Only 1200 °C extraction above blank level.
[b]In cm^3 STP g^{-1}.

et al. (2016) as well as recently reported ages of NWA 7325 that are based on other systems, which are old (U-Pb age 4562.5 ± 4.4 Ma, Amelin et al. 2013; Pb-Pb age 4563.4 ± 2.6 Ma, Koefoed et al. 2016; Al-Mg age 4563.09 ± 0.26 Ma, Koefoed et al. 2016).

In summary, due to the low K-content (19 ppm), high Ca-content (CaO 17.4%, in reasonable agreement with bulk data of Irving et al. 2013), and large amount of cosmogenic Ar, a precise Ar-Ar age is difficult to determine. The integrated Ar-Ar age of NWA 7325 appears ancient (4435 ± 87 Ma) if corrected for a solar-type $^{40}Ar/^{36}Ar$ composition of 1 ± 1. However, accounting for the apparent presence of atmospheric argon, a more reliable much younger lower age limit of 3200 ± 260 Ma is calculated and regarded as an upper age limit for a late thermal event.

Cosmic-Ray Exposure Age Derived by $^{38}Ar/^{37}Ar_{Ca}$ Ratios

In the Ar-Ar dating experiment, we observe a significant cosmogenic $^{38}Ar_C$ content of 4.029×10^{-8} cm^3 STP g^{-1}. This agrees well with the result of the noble gas measurements for the second whole rock split (4.394×10^{-8} cm^3 STP g^{-1}). The dominant cosmogenic ^{38}Ar contribution in our sample is from Ca, as the production ratio of cosmogenic ^{38}Ar derived by Ca and Fe (the second most important target element in NWA 7325) is about 20 (Eugster and Michel 1995), and the Ca/Fe ratio in the bulk sample of 10.5 (Irving et al. 2013) adds another order of magnitude. Hence, a comparison of cosmogenic $^{38}Ar_C$ and neutron-induced Ca-derived ^{37}Ar can be used to derive a cosmic-ray exposure age. In fact, we observe a well-defined age "plateau" (in $^{38}Ar_{COSM}/^{37}Ar_{Ca}$ versus fractional release of ^{37}Ar in %) for the 900–1700 °C extractions (eight steps, Fig. 2C) encompassing 98% of the ^{37}Ar release. Knowledge of an appropriate production rate of cosmogenic ^{38}Ar from Ca accordingly allows calculation of an exposure age.

The respective production rate depends on the shielding of the sample during its burial in the host meteoroid though this dependency is minor in the case of $^{38}Ar_C$ production and therefore, the choice of $(^{22}Ne/^{21}Ne)_C$ for evaluation is not crucial. For the calculation of production rates, we take the $(^{22}Ne/^{21}Ne)_C$ shielding factor obtained in our noble gas analyses (see the Noble Gas Composition and CRE Ages from Cosmogenic ^3He, ^{21}Ne and ^{38}Ar Abundances in Nonirradiated Whole Rock Splits section) of 1.209 (wr#2), neglect again any solar cosmic ray (SCR) component, and use the formalism of Eugster and Michel (1995) as applicable to eucrites. Finally, we take the chemical composition of the meteorite (reported by Irving et al. 2013). We obtain a production rate of 2.33×10^{-9} cm^3 STP $(g \times Ma)^{-1}$. Normalizing to the Ca-content of (12.40 ± 0.15) % computed from $^{37}Ar_{Ca}$, a plateau age for the cosmic-ray exposure, from the 900 to 1700 °C extractions ($n = 8$), is (17.45 ± 0.12) Ma. However, this age is similar to the exposure age of 18.8 ± 1.0 Ma reported by Weber et al. (2016), which seems to be fortuitous. This is because for calculating

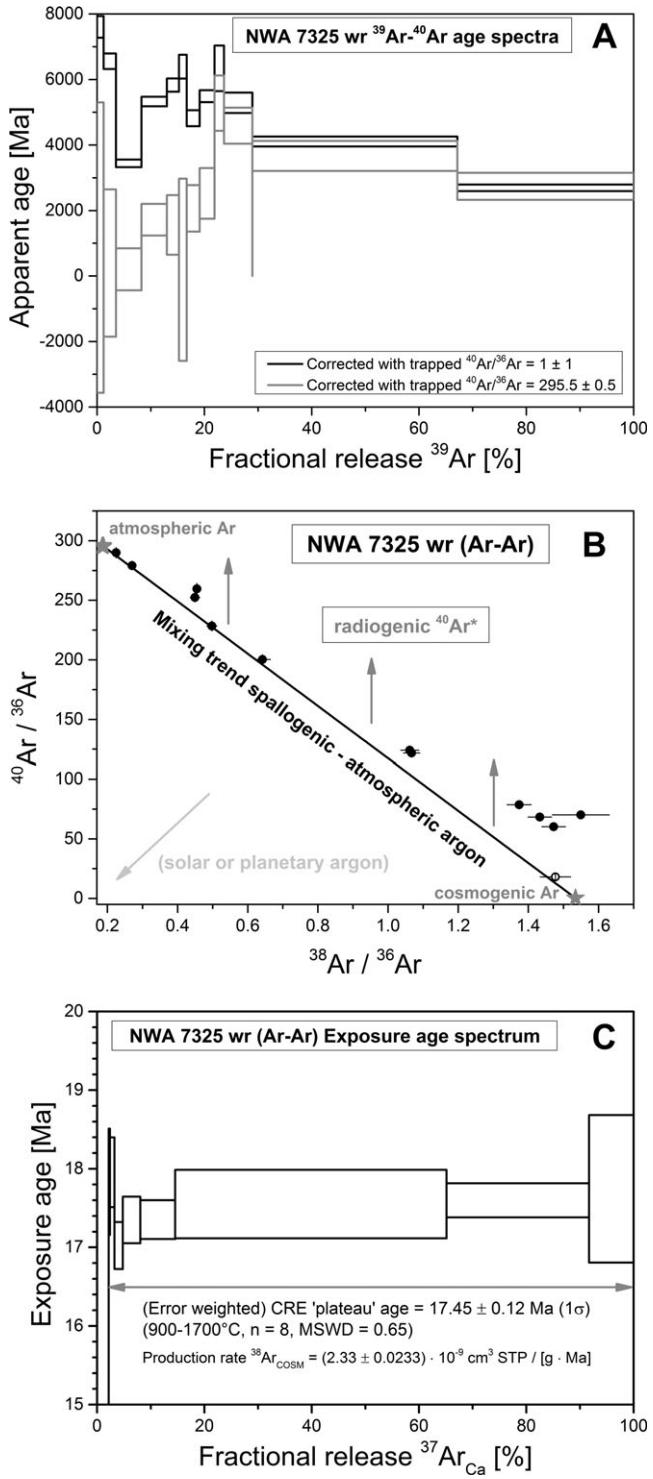

Fig. 2. A) ^{39}Ar-^{40}Ar age spectra of NWA 7325 obtained with two different assumptions on the trapped composition used for correction: solar (or planetary) ^{40}Ar/^{36}Ar = 1 ± 1 (black spectrum) and atmospheric ^{40}Ar/^{36}Ar = 295.5 ± 0.5 (Steiger and Jäger 1977) (gray spectrum). B) Argon three-isotope diagram of results from our ^{40}Ar/^{39}Ar study. Apparently, all data plot along or slightly above a mixing trend between atmospheric and cosmogenic Ar. No clear contributions from solar or planetary argon can be resolved. See text for details. C) Exposure age versus fractional release of Ca-derived ^{37}Ar. An age plateau encompassing 98% of the ^{37}Ar-release is observed. The plateau age of 17.45 ± 0.12 Ma (statistical uncertainty) refers to a production rate of 2.33×10^{-9} cm^3 STP (g × Ma)$^{-1}$, equivalent to a shielding parameter $(^{22}Ne/^{21}Ne)_{COSM}$ = 1.209 (calculated after Eugster and Michel 1995).

the ^{38}Ar CRE age, Weber et al. (2016) used the formalism of Eugster (1988) and Schultz et al. (1991) for chondritic lithologies (note, they do not specify the assumed shielding). Because their given Mg/(Al+Si) ratio of 0.17 is far below a chondritic composition, we performed a recalculation with the same formalism used in our study, i.e., following Eugster and Michel (1995). This resulted in significantly lower age values of 13.5–13.9 Ma (Supplementary Material 5 in supporting information). Both this value and our value of 17.5 Ma are based on Ca-contents determined from Ar-Ar measurements, which commonly are considered as robust. In the Evidence for Sample Heterogeneities section we discuss the discrepant ages in more detail.

Iodine–Xenon Dating Results

An irradiated whole rock piece of NWA 7325 was analyzed in an attempt to derive a ^{129}I-^{129}Xe age. Xenon, in particular in low- and medium-temperature steps (800–1400 °C), showed clear signals of (neutron-induced) fissiogenic xenon ($^{131}Xe_{fiss}$, $^{132}Xe_{fiss}$, $^{134}Xe_{fiss}$, $^{136}Xe_{fiss}$), bariogenic $^{131}Xe_{Ba,}$ and iodogenic $^{128}Xe_I$ (Table 1). Fission contributions appear solely due to the neutron-induced fission of ^{235}U during irradiation. No contributions of fissiogenic Xe from ^{238}U or ^{244}Pu are detected, as can be seen in a diagram ^{130}Xe/^{132}Xe versus ^{134}Xe/^{132}Xe (Fig. S1 in Supplementary Material 4). Iodogenic ^{128}Xe was not supported by excesses of radiogenic ^{129}Xe* (Fig. 3A), which is equivalent with either resetting of the ^{129}I-^{129}Xe clock after several half-lives of ^{129}I ($t_{1/2}$ = 15.7 Ma, Pravdivtseva et al. 2017a, 2017b) or a relatively recent addition of (stable) iodine. It is possible, however, to estimate a lower age limit from the highest observed $^{129}Xe^*/^{128}Xe_I$ ratio of 0.2463 (1450 °C extraction, equivalent to steepest possible trend of an "isochron," gray line in Fig. 3A). With a $^{129}Xe^*/^{128}Xe_I$ ratio of the co-irradiated Shallowater meteorite of 0.7777 ± 0.0059 (1σ), we obtain for NWA 7325 an age offset of 26.0 Ma younger than Shallowater. With a Shallowater reference age of 4562.4 ± 0.2 Ma (Pravdivtseva et al. 2017a, 2017b), this translates into a lower absolute age limit of about 4536 Ma.

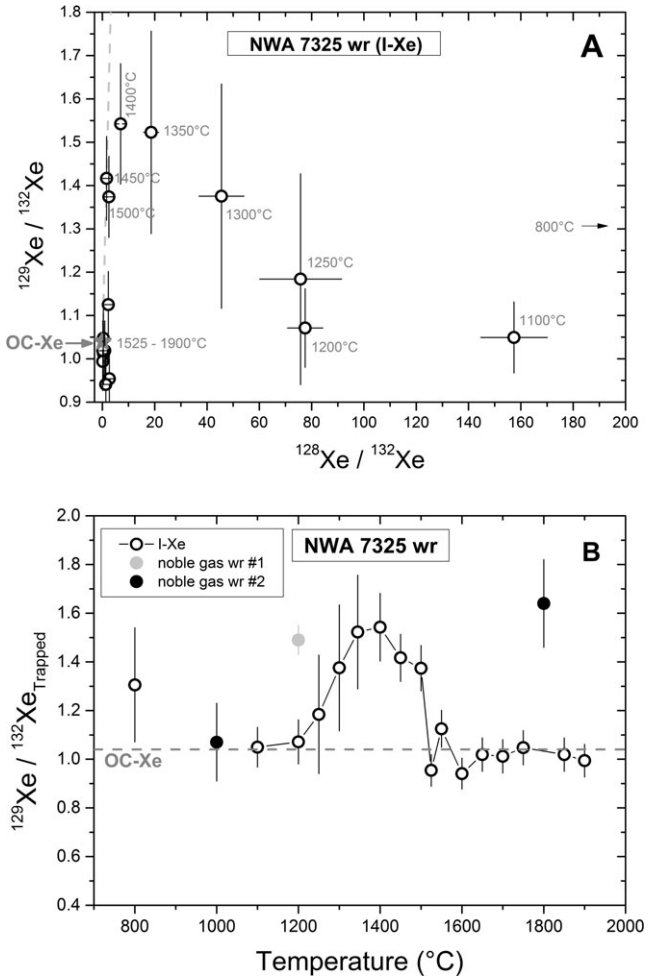

Fig. 3. A) Xenon three-isotope diagram $^{129}Xe/^{132}Xe$ versus $^{128}Xe/^{132}Xe$. No isochron relation is observed. Assuming the highest $^{129}Xe^*/^{128}Xe_I$ ratio (equivalent to construction of trend with steepest slope possible from data, gray stippled line), we can calculate a lower I-Xe age limit of 4536 Ma. B) $^{129}Xe/^{132}Xe$ ratios versus temperature for three experiments (I-Xe, St. Louis; noble gases Heidelberg). The highest ratios are observed at the major release peak.

Major degassing of radiogenic $^{129}Xe^*$ occurred at 1300–1450 °C and is associated with an increase of $^{129}Xe/^{132}Xe$ ratios (Fig. 3B). With the highest value of fission-corrected $^{129}Xe/^{132}Xe = 1.54 \pm 0.14$ observed at 1400 °C, this is suggestive of a single carrier phase. In an Arrhenius-type diagram of fractional release of radiogenic $^{129}Xe^*$ (1100–1450 °C extractions, Fig. S2 in Supplementary Material 4), i.e., ^{129}Xe corrected for a trapped Xe component having ordinary chondrite Xe composition ($^{129}Xe/^{132}Xe = 1.0399 \pm 0.0025$ [1σ], Lavielle and Marti 1992), a reasonably well-defined linear trend is observed. Calculation of precise diffusion parameters, however, is hampered by uncertainties in absolute temperature measurements (see Supplementary Material 4) and therefore is too imprecise to gather more information about the carrier phase of radiogenic $^{129}Xe^*$. The observed elevated $^{129}Xe/^{132}Xe$ ratios are in agreement with xenon data derived from our nonirradiated whole rock splits (see the next section). They are similar to ratios reported by Hasegawa et al. (2014) and Weber et al. (2016), and can be similarly interpreted to indicate an old I-Xe age of NWA 7325, possibly equivalent with its U-Pb age, but reflecting signs of later isotopic re-equilibration.

Noble Gas Composition and CRE Ages From Cosmogenic ^{3}He, ^{21}Ne, and ^{38}Ar Abundances in Nonirradiated Whole Rock Splits

All noble gases show significant cosmic-ray–induced isotopic shifts: High $^{3}He/^{4}He$, high $^{21}Ne/^{22}Ne$ (Fig. 4), and high $^{38}Ar/^{36}Ar$ ratios as well as in Kr clear overabundances of, e.g., ^{83}Kr. Hence, it is difficult to deduce information about the trapped compositions, in particular since the deviations from cosmogenic compositions can be easily explained by addition of low amounts of terrestrial atmospheric noble gases. An exception is the xenon system, which shows a clear ^{129}Xe excess from short-lived ^{129}I (half-life 15.7 Ma, Pravdivtseva et al. 2017a, 2017b) with $^{129}Xe/^{132}Xe$ ratios up to 1.64 ± 0.18 (1σ), in agreement with our results discussed in the Iodine–Xenon Dating Results section and those reported by Hasegawa et al. (2014) and Weber et al. (2016). Therefore, we mainly focus here on a discussion of cosmogenic isotopes and associated cosmic-ray exposure ages.

The shielding parameter $(^{22}Ne/^{21}Ne)_C$ is 1.188 ± 0.014 (wr1) and 1.209 ± 0.003 (wr2), but shows a slight variation in course of the heating process. This probably mirrors the differing mineral chemistry and hence, varying production rates of cosmogenic isotopes in the respective carrier phases which differ in their degassing properties. It is also reflected in different production rates for different element systems, e.g., ^{21}Ne and ^{38}Ar. For example, ^{21}Ne production is dominated by reactions of cosmic rays with Mg, Al, and Si, whereas ^{38}Ar is dominantly produced by cosmic-ray–interaction with Ca (interaction with other elements is negligible due to low production rates [e.g., Fe] or concentrations [e.g., K] or both, as for Ti). Following the approach of Garrison et al. (1995) and Eugster et al. (1997), we may deduce the presence of neon isotopes produced by SCR from the relation between Mg/(Al+Si) ratio and $(^{22}Ne/^{21}Ne)_C$. In such a diagram (like fig. 1 in Eugster et al. 1997), NWA 7325 plots within the field dominated entirely by galactic cosmic-ray–induced neon production. Hence, we neglect any possible contribution of SCR-induced production. In analogy to chondritic lithologies, values of both

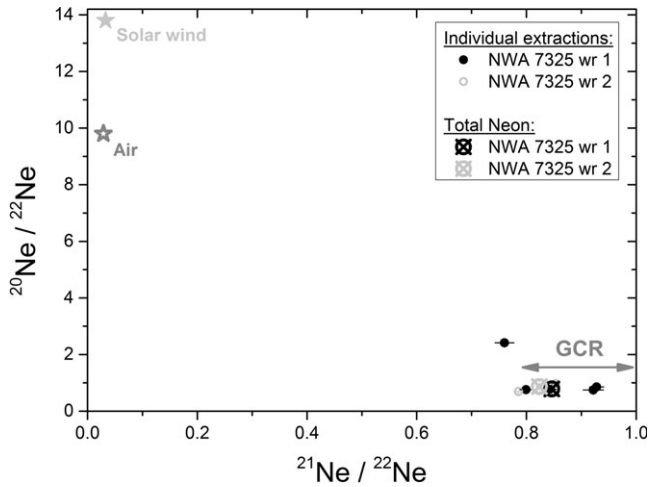

Fig. 4. Neon three-isotope diagram, demonstrating the highly cosmogenic character of the neon composition. Errors represent 1σ-uncertainties.

shielding parameters point to a rather small meteoroid size of a few decimeters only, but the depth dependency of the shielding parameter in achondrites is less constrained. Based on the shielding parameter, the bulk composition reported by Irving et al. (2013) and the amounts of cosmogenic ^{3}He, ^{21}Ne, and ^{38}Ar, we calculated CRE ages based on the empirical relations given by Eugster and Michel (1995). We chose their equations for eucrites because eucritic Mg/(Al+Si) ratios (approximately 0.16) are similar to that of NWA 7325 (Mg/(Al+Si) = 0.23, Irving et al. 2013). Note that Eugster et al. (1997) applied eucritic CRE production rates to the Martian meteorite Zagami which has essentially the same Mg/(Al+Si) ratio (=0.238) as NWA 7325. Resulting ^{3}He, ^{21}Ne, and ^{38}Ar CRE ages of NWA 7325 wr1 are 7.2, 10.9, and 6.4 Ma. This differs markedly from NWA 7325 wr#2, for which we obtain ^{3}He, ^{21}Ne, and ^{38}Ar CRE ages of 13.0, 25.6, and 18.9 Ma, respectively. Whole rock sample #2 agrees reasonably well with the $^{38}Ar_C$ CRE age obtained from our irradiated sample (plateau age 17.5 Ma), which is more reliable due to its known Ca-content. This indicates a similar Ca-content of these two whole rock splits. However, the higher $^{21}Ne_C$ CRE age (compared to the age based on $^{38}Ar_C$) asks for an explanation. Since the main target elements of cosmogenic ^{21}Ne production are Mg, Al, and Si, identical ^{21}Ne and ^{38}Ar CRE ages might be obtained by adjusting the (assumed) chemical composition. The calculated ^{21}Ne CRE age depends on the relative proportions of the major mineral constituents, forsterite, diopside, and anorthite. We therefore have assessed the impact of the modal compositions on the ^{21}Ne CRE age (see Supplementary Material 5), under the assumption of a constant Ca-content equivalent to the whole rock composition defined by the results of our Ar-Ar measurement (=12.4 wt% Ca), thus keeping the ^{38}Ar CRE age of 17.5 Ma (see the Cosmic-Ray Exposure Age Derived by $^{38}Ar/^{37}Ar_{Ca}$ Ratios section). Doing so, in a simplified ternary system (forsterite, diopside, and anorthite), we have modeled the ^{21}Ne CRE age as a function of the modal anorthite content. It turns out that a whole rock composition of $An_{10}Di_{59}Fo_{31}$ would bring the ^{21}Ne CRE age in agreement with the ^{38}Ar CRE age of 17.5 Ma. However, this modal composition would strongly differ from its previously reported average composition, e.g., leading to a drop of the anorthite content by a factor of about 5, which appears unlikely. Furthermore, this modal composition would be more similar to a chondritic composition. Hence, calculation of cosmic-ray exposure ages would again require a formalism applicable to chondritic compositions (Eugster 1988; Schultz et al. 1991). The resulting ^{21}Ne and ^{38}Ar CRE ages then are 22.2 Ma and 34.0 Ma, respectively.

We have also tried to recalculate in a similar manner CRE ages obtained for NWA 7325 wr1, which for all cosmogenic isotopes showed much lower CRE-ages than NWA 7325 wr2 and the irradiated whole rock split in our Ar-Ar analysis. If we neglect Fe as a target element for production of $^{38}Ar_C$, leaving Ca as the only important target element, a much lower nominal Ca-content of only 4.7 wt% would be required to result in a ^{38}Ar CRE age of 17.5 Ma. If we try to adjust the ^{21}Ne CRE age of NWA 7325 wr1 by changing the modal composition according to a constant Ca of 12.4% in the same ternary system as for NWA 7325 wr2, the maximum ^{21}Ne CRE age that can be achieved is only 11.2 Ma, for $An_{86}Fo_{14}$ and no diopside (any addition of diopside at the expense of anorthite would lower the age). With assumption of a much lower Ca-content in NWA 7325 wr1 of 4.7% (as assessed from ^{38}Ar CRE age calculation), we obtain a maximum ^{21}Ne CRE age of 5.8 Ma with a modal composition of $An_{32.6}Fo_{67.4}$. If, as an alternative, we model the binary system diopside–forsterite only, this is restricted by the required Ca-contents of 4.7% (assessed by ^{38}Ar CRE-age from same split), 12.4% (from Ar-Ar analyses) or 12.8% (from bulk composition given by Irving et al. 2013). In the former case, this would be equivalent to 25.4% of diopside and results in a ^{21}Ne CRE age of 5.2 Ma. For Ca-contents of 12.4% and 12.8%, we calculate ^{21}Ne CRE ages of 7.2 Ma and 7.3 Ma, and diopside contents of 67% and 69%, respectively. In a final attempt, we have also inserted an alternative bulk Ca-content of 15.9% into our calculation, equivalent to the modal composition $An_{54}Di_{44}Fo_2$ reported in Weber et al. (2016) based on modal compositions derived from

a thin section. In this case, the ^{21}Ne CRE ages would be 11.8 Ma (wr1) and 27.7 Ma (wr2). Note that the analyzed whole rock split by Weber et al. (2016) utilizing the ^{37}Ar-^{38}Ar method had a Ca-content of 11.3% only, similar to the content obtained from our own Ar-Ar analysis. This demonstrates that element concentrations derived from microprobe data or calculated with modal compositions not necessarily agree with element contents of larger splits typically used for noble gas measurements (this does not change by considering a more realistic anorthite content of 88% in plagioclase only). To summarize, in the case of NWA 7325 wr1, it is not possible to adjust both the ^{21}Ne and ^{38}Ar CRE age to a value of 17.5 Ma by simple changes in the assumed chemical composition.

Finally, the differing but systematically lower ^{3}He CRE ages of both splits compared with ^{21}Ne and ^{38}Ar CRE ages are difficult to explain by simple variation of the modal mineral composition because ^{3}He production depends only very weakly on chemical composition. Thus, weathering-induced preferential loss of He relative to the other noble gases seems a better explanation. In such a scenario, one might expect a corresponding loss of Ne and Ar as well, with Ne more likely to escape the meteorite. However, this is in contradiction to the apparently higher ^{21}Ne CRE ages compared with the ^{38}Ar CRE ages, which is observed for both whole rock splits.

Evidence for Sample Heterogeneities

The CRE-exposure ages calculated for both splits and with different cosmogenic nuclides differ significantly from each other and from the results of Weber et al. (2016), if the different calculation procedures are taken into account. In addition, we observe different concentrations of trapped ^{132}Xe obtained in this study, Hasegawa et al. (2014), and Weber et al. (2016). Simple explanations of the discrepant results between both whole rock splits appear unsatisfactory, e.g., a weighing error of >100 mg is extremely unlikely. Terrestrial alteration is another possibility to lose cosmogenic gases from a sample. However, in this case we would also expect a larger contribution from atmospheric noble gases which is at odds with the rather similar isotopic composition observed for NWA 7325 (Fig. 4; Tables 2 and 4). We may partly attribute the different noble gas concentrations to their distinctive degassing behavior during atmospheric transit. The ratios of concentrations of cosmogenic ^{3}He, ^{21}Ne, ^{38}Ar, and trapped ^{132}Xe between nonirradiated splits wr2 and wr1 appear to increase with atomic weight (ratios are approximately 1.8, 2.3, 3.0, and 3.9, respectively). This is opposite to expectation if late partial degassing caused the differences in concentrations for which we would expect a higher loss of the light noble gases compared with the heavy noble gases. Alternatively, a change in mineralogical composition and hence, deviations from, the average chemical composition provided by Irving et al. (2013) may have led to some of the observed age differences. This has been discussed in detail in the subsection Noble Gas Composition and CRE Ages From Cosmogenic ^{3}He, ^{21}Ne, and ^{38}Ar Abundances in Nonirradiated Whole Rock Splits section for intrasample variations in ^{21}Ne and ^{38}Ar CRE-ages of NWA 7325 wr2. However, this can neither explain the differences between the (recalculated) ^{38}Ar CRE-ages reported by Weber et al. (2016) and that obtained in our Ar-Ar study, nor the age differences observed between the two nonirradiated splits in this study. Trapped ^{132}Xe concentrations of the irradiated whole rock split NWA 7325 wr-I-Xe (Table 1) are similar to concentrations found in NWA 7325 wr2 and also are similar to ^{132}Xe concentrations reported in Weber et al. (2016). Furthermore, trapped ^{132}Xe concentrations of (2.4–3.1) $\times$ 10^{-11} cm^3 STP g^{-1} have been reported by Hasegawa et al. (2014) that are within the concentration range observed in our study (wr1: 1.0 $\times$ 10^{-11}, wr2: 3.9 $\times$ 10^{-11}, wr-I-Xe: 3.7 $\times$ 10^{-11}, in cm^3 STP g^{-1}). Similarly, amounts of cosmogenic ^{38}Ar derived from our Ar-Ar study and NWA 7325 wr2 differ by <10%. Our nonirradiated split NWA 7325 wr1 shows the lowest concentration of cosmogenic and trapped nuclides of all samples. We conclude that the only remaining solution to the observed large variation in concentrations and CRE-ages is an existing heterogeneity in noble gas distribution within NWA 7325.

SUMMARY AND CONCLUSIONS

We determined an integrated Ar-Ar age of 4435 $\pm$ 87 Ma (assuming an initial solar-type ^{40}Ar/^{36}Ar of 1 $\pm$ 1) suggestive of an early closure of the K-Ar system, which would be in agreement with other Ar-Ar ages (Weber et al. 2016) and ancient U-Pb, Pb-Pb, and Al-Mg ages of about 4563 Ma (Amelin et al. 2013; Koefoed et al. 2016). However, accounting for the apparent presence of atmospheric argon results in a calculated minimum age of 3200 $\pm$ 260 Ma. This age would represent an upper age constraint for a last severe Ar-loss event, possibly related to impact heating. A ^{38}Ar cosmic-ray exposure plateau age of 17.45 $\pm$ 0.12 Ma (only statistical error) could be derived from measured $^{38}Ar_C/^{37}Ar_{Ca}$ ratios of the 900–1700 °C extractions (N = 8) and the total Ca-content (12.4 wt%), applying the formalism of Eugster and

Michel (1995) for eucrites ($^{38}Ar_C$ production rate = 2.33×10^{-9} cm^3 STP [g × Ma]$^{-1}$). No discernible ^{129}I-^{129}Xe age could be determined in spite of an existing ^{129}Xe excess. From the highest observed $^{129}Xe^*/^{128}Xe_I$ ratio, we derive a lower limit for the I-Xe age of 4536 Ma.

Noble gas isotopic compositions of two nonirradiated splits of NWA 7325 are similar to each other and are dominated by cosmogenic isotopes, except for Xe (Kr data were obtained for one of the splits only, where also cosmogenic contributions are apparent). The elevated $^{129}Xe/^{132}Xe$ ratios (up to 1.65 ± 0.18) observed in our study and reported by Hasegawa et al. (2014) and Weber et al. (2016) imply the presence of short-lived ^{129}I (half-life 15.7 Ma) during formation of this cumulate rock and thus an early formation, again in agreement with results from other chronometers. The shielding parameters $(^{22}Ne/^{21}Ne)_C$ of 1.188 (split 1) and 1.209 (split 2) point to a small radius of the parent meteoroid of a few decimeters. Concentrations of noble gases in two nonirradiated whole rock splits NWA 7325 wr1 and wr2 differed by more than a factor of 2. This results in different cosmic-ray exposure ages even when allowing for possible differences in chemical composition. Intrasample variations of ^{21}Ne and ^{38}Ar CRE-ages in NWA 7325 wr2 calculated with a nominal whole rock chemistry (Irving et al. 2013), on the other hand, can be resolved by adjusting the modal composition of this sample, but requiring unrealistic modal compositions. Within uncertainties, the ^{38}Ar CRE-age of NWA 7325 wr2 is similar to the CRE-age of 17.5 Ma derived from the Ar-Ar analysis. Nominally this is similar to the 19 ± 1 Ma CRE-age reported by Weber et al. (2016), but these authors used different calculation procedures. If recalculated with the production rate formalism used in this study, the ^{38}Ar cosmic-ray exposure age of Weber et al. (2016) decreases to 13.5–14 Ma.

The oxygen isotopic composition of NWA 7325 resembles the oxygen isotopic trends of ureilites, winonaites, and acapulcoites/lodranites (Irving et al. 2013). Though, from petrologic evidence, this coincidence is considered as fortuitous (e.g., Irving et al. 2013; El Goresy et al. 2014; Goodrich et al. 2014), we nonetheless may compare the CRE-age of NWA 7325 with CRE-ages reported for these meteorite groups. Doing so, it should be kept in mind that CRE-ages only reflect breakup of small fragments from a potentially much larger parent body. Hence, the CRE-age distributions of different meteorite populations are certainly biased by small-scale processes on a parent body. The acapulcoite/lodranite group reveals a well-confined cluster of CRE-ages at about 7 Ma (Terribillini et al. 2000), significantly younger than the CRE-age of NWA 7325 and thus, the latter is unlikely to be derived by the same ejection event. CRE-ages of ureilites range up to 35 Ma and show a slight (though statistically not significant) overabundance in the age range of 20-30 Ma (Eugster 2003). More recently, however, it was shown that no age clustering of CRE-age of ureilites is apparent from age data (Beard and Swindle 2017). Hence, the CRE-age of NWA 7325 could agree with ureilite CRE-ages, but this is not conclusive. This is also the case for the winonaites which have reported CRE-ages of 20–80 Ma (Benedix et al. 1998). In essence, judging from the distribution of cosmic-ray exposure ages alone, we consider the acapulcoite/lodranite parent body as an unlikely source of NWA 7325, whereas the ureilite or winonaite parent bodies cannot be excluded.

Acknowledgments—The authors thank Deutsche Forschungsgemeinschaft for funding (grant numbers TR333/13 and HO2591/4) and the Klaus-Tschira-Stiftung gGmbH for financial support. This work greatly benefitted from discussions with Winfried Schwarz. Johannes Grimm is acknowledged for his technical support during the electron microprobe analysis. We thank Tim Swindle and Kees Welten for constructive reviews which improved this manuscript.

Editorial Handling—Dr. Marc Caffee

REFERENCES

Amelin Y., Koefoed P., Iizuka T., and Irving A. J. 2013. U-Pb age of ungrouped achondrite NWA 7325. 76th Annual Meteoritical Society Meeting, abstract # 5165.

Barrat J. A., Greenwood R. C., Verchovsky A. B., Gillet P., Bollinger C., Langlade J. A., Liorzou C., and Franchi I. A. 2015. Crustal differentiation in the early solar system: Clues from the unique achondrite Northwest Africa 7325 (NWA 7325). *Geochimica et Cosmochimica Acta* 168:280–292.

Beard S. P. and Swindle T. D. 2017. Search for evidence of source event grouping among ureilites. *Meteoritics & Planetary Science* 52:2343–2352.

Benedix G. K., McCoy T. J., Keil K., Bogard D. D., and Garrison D. H. 1998. A petrologic and isotopic study of winonaites: Evidence for early partial melting, brecciation, and metamorphism. *Geochimica et Cosmochimica Acta* 62:2535–2553.

Bischoff A., Ward D., Weber I., Morlok A., Hiesinger H., and Helbert J. 2013. NWA 7325—Not a typical olivine gabbro, but a rock experienced fast cooling after a second (partial) melting. European Planetary Science Congress 8, EPSC2013-427 (abstract).

Brereton N. R. 1970. Corrections for interfering isoptopes in the ^{40}Ar-^{39}Ar-dating method. *Earth and Planetary Science Letters* 8:427–433.

Dunlap D. R., Wadhwa M., and Romaneillo S. R. 2014. ^{26}Al-^{26}Mg systematics in the unusual ungrouped

achondrite NWA 7325 and the eucrite Juvinas (abstract #2186). 45th Lunar and Planetary Science Conference. CD-ROM.

El Goresy A., Nakamura T., Miyahara M., Ohtani E., Gillet P., Jogo K., Yamanobe M., and Ishida H. 2014. The unique differentiated meteorite NWA7325: Highly reduced, stark affinities to E-chondrites and unknown parental planet. 77th Annual Meteoritical Society Meeting, abstract #5028.

Eugster O. 1988. Cosmic-ray production rates for ^{3}He, ^{21}Ne, ^{38}Ar, ^{83}Kr, and ^{126}Xe in chondrites based on ^{81}Kr-Kr exposure ages. *Geochimica et Cosmochimica Acta* 52:1649–1662.

Eugster O. 2003. Cosmic-ray exposure ages of meteorites and lunar rocks and their significance. *Chemie der Erde* 63:3–30.

Eugster O. and Michel T. 1995. Common asteroid break-up events of eucrites, diogenites, and howardites and cosmic-ray production rates for noble gases in achondrites. *Geochimica et Cosmochimica Acta* 59:177–199.

Eugster O., Weigel A., and Polnau E. 1997. Ejection times of Martian meteorites. *Geochimica et Cosmochimica Acta* 61:2749–2757.

Garrison D. H., Rao M. N., and Bogard D. D. 1995. Solar-proton produced neon in shergottite meteorites and implications for their origin. *Meteoritics* 30:738–747.

Goodrich C. A., Kita N. T., and Nakashima D. 2014. Petrology of the NWA 7325 ungrouped achondrite—Meteorite from Mercury, the ureilite parent body, or a previously unsampled asteroid? (abstract #1246). 45th Lunar and Planetary Science Conference. CD-ROM.

Hasegawa H., Haba M. K., Nagao K., Mikouchi T., and Bizzarro M. 2014. Noble gas and mineralogical studies of NWA 7325 ungrouped achondrite. 77th Annual Meteoritical Society Meeting, abstract #5306.

Hohenberg C. M. 1980. High sensitivity pulse-counting mass spectrometer system for noble gas analysis. *Review of Scientific Instruments* 51:1075–1082.

Irving A. J., Kuehner S. M., Bunch T. E., Ziegler K., Chen G., Herd C. D. K., Conrey R. M., and Ralew S. 2013. Ungrouped mafic achondrite Northwest Africa 7325: a reduced, iron-poor cumulate olivine gabbro from a differentiated planetary body (abstract #2164). 44th Lunar and Planetary Science Conference. CD-ROM.

Jabeen I., Ali A., Banerjee N. R., Osinski G., Ralew S., and DeBoer S. 2014. Oxygen isotope compositions of mineral separates from NWA 7325 suggest a planetary (Mercury?) origin (abstract #2215). 45th Lunar and Planetary Science Conference. CD-ROM.

Kita N. T., Sanborn M. E., Yin Q.-Z., and Goodrich C. A. 2014. The NWA 7325 ungrouped achondrite—Possible link to ureilites? Oxygen and chromium isotopes and trace elements abundances (abstract #1455). 45th Lunar and Planetary Science Conference. CD-ROM.

Koefoed P., Amelin Y., Yin Q.-Z., Wimpenny J., Sanborn M. E., Iizuka T., and Irving A. J. 2016. U-Pb and Al-Mg systematics of the ungrouped achondrite Northwest Africa 7325. *Geochimica et Cosmochimica Acta* 183:31–45.

Lämmerzahl P. and Zähringer J. 1966. K-Ar Altersbestimmungen an Eisenmeteoriten—II Spallogenes ^{40}Ar und ^{40}Ar-^{38}Ar-Bestrahlungsalter. *Geochimica et Cosmochimica Acta* 30:1059–1074.

Lavielle B. and Marti K. 1992. Trapped xenon in ordinary chondrites. *Journal of Geophysical Research* 97:20,875–20,881.

Lee J.-Y., Marti K., Severinghaus J. P., Kawamura K., Yoo H.-S., Lee J. B., and Kim J. S. 2006. A redetermination of the isotopic abundances of atmospheric Ar. *Geochimica et Cosmochimica Acta* 70:4507–4512.

Ozima M. and Podosek F. A. 1983. *Noble gas geochemistry*. Cambridge: Cambridge University Press. 367 p.

Pravdivtseva O., Meshik A., Hohenberg C. M., and Krot A. N. 2017a. I-Xe systematics of the impact plume produced chondrules from the CB carbonaceous chondrites: Implications for the half-life value of 129I and absolute age normalization of 129I–129Xe chronometer. *Geochimica et Cosmochimica Acta* 201:320–330.

Pravdivtseva O., Meshik A., and Hohenberg C. M. 2017b. Evaluation of the ^{129}I half-life value through analyses of primitive meteorites. *Proceedings of the 14th International Symposium on Nuclei in the Cosmos (NIC2016), JPS Conference Proceedings* 14:011005.

Renne P. R., Balco G., Ludwig K. R., Mundil R., and Min K. 2011. Response to the comment by W.H. Schwarz et al. on "The joint determination of the 40K decay constants 40Ar*/40K in Fish Canyon sanidine standard, and improved accuracy for 40Ar/39Ar geochronology" by Paul R. Renne et al. (2010). *Geochimica et Cosmochimica Acta* 75:5097–5100.

Sanborn M. E., Yamakawa A., Yin Q.-Z., Irving A. J., and Amelin Y. 2013. Chromium isotopic studies of ungrouped achondrites NWA 7325, NWA 2976, and NWA 6704. 76th Annual Meteoritical Society Meeting, abstract #5220.

Schultz L., Weber H. W., and Begemann F. 1991. Noble gases in H-chondrites and potential differences between Antarctic and non-Antarctic meteorites. *Geochimica et Cosmochimica Acta* 55:59–66.

Schwarz W. H. and Trieloff M. 2007. Intercalibration of ^{40}Ar-^{39}Ar age standards NL-25, HB3gr hornblende, GA1550, SB-3, HD-B1 biotite and BMus/2 muscovite. *Chemical Geology* 242:218–231.

Schwarz W. H., Kossert K., Trieloff M., and Hopp J. 2011. Comment on "The joint determination of the ^{40}K decay constants ^{40}Ar*/^{40}K in Fish Canyon sanidine standard, and improved accuracy for ^{40}Ar/^{39}Ar geochronology" by Paul R. Renne et al. (2010). *Geochimica et Cosmochimica Acta* 75:5094–5096.

Steiger R. H. and Jäger E. 1977. Subcommission on geochronology: Convention on the use of decay constants in geo- and cosmochronology. *Earth and Planetary Science Letters* 36:359–362.

Sutton S. R., Wirick S., and Goodrich C. A. 2014. Ungrouped achondrite NWA 7325: Titanium, vanadium and chromium XANES of mafic silicates record highly-reduced origin (abstract #1275). 45th Lunar and Planetary Science Conference. CD-ROM.

Terribillini D., Eugster O., Herzog G. F., and Schnabel C. 2000. Evidence for common break-up events of the acapulcoites-lodranites and chondrites. *Meteoritics & Planetary Science* 35:1043–1050.

Turner G. 1971. ^{40}Ar-^{39}Ar-dating: The optimisation of irradiation parameters. *Earth and Planetary Science Letters* 10:227–234.

Weber I., Morlok A., Bischoff A., Hiesinger H., and Helbert J. 2014. Mineralogical and spectroscopic studies on NWA 7325 as an analogue sample for rocks from Mercury (abstract #1323). 45th Lunar and Planetary Science Conference. CD-ROM.

Weber I., Morlok A., Bischoff A., Hiesinger H., Ward D., Joy K. H., Crowther S. A., Jastrzebski N. D., Gilmour J. D., Clay P. L., Wogelius R. A., Greenwood R. C., Franchi I. A., and Münker C. 2016. Cosmochemical and spectroscopic properties of Northwest Africa 7325 – A consortium study. *Meteoritics & Planetary Science* 51:3–30.

Weider S. Z., Nittler L. R., Starr R. D., McCoy T. J., Stockstill-Cahill K. R., Byrne P. K., Denevi B. W., Head J. W., and Salomon S. C. 2012. Chemical heterogeneity on Mercury's surface revealed by the MESSENGER X-ray spectrometer. *Journal of Geophysical Research* 117:E00L05.

SUPPORTING INFORMATION

Additional supporting information may be found in the online version of this article:

Table S1. Microprobe results of NWA 7325.

Table S2. Results of Ar-Ar dating.

Table S3. Modeling the CRE age as a function of modal composition.

Data S1. Back-scattered electron microscope images.

Data S2. Supplementary analytical details and figures.